ACTIVATION OF FAULT SYSTEMS BEFORE RECENT LARGEST EARTHQUAKES WORLDWIDE

[1,2]KOSSOBOKOV, V. G., [1,3]KEILIS-BOROK, V. I., [1]ROMASHKOVA, L. L. [1]International Institute of Earthquake Prediction Theory and Mathematical Geophysics, Russian Ac. Sci., Moscow, Russian Federation, [2]Institut de Physique du Globe de Paris, France, [3]Institute of Geophysics and Planetary Physics, University of California, Los Angeles, USA.

Summary. Seismic process is an essential part in dynamics of the lithosphere. The later is viewed as a self-organized hierarchy of blocks and faults of different sizes. Earthquakes evidently cascade into aftershocks that re-adjust the system in the locality of the main shock rupture. Our systematic analysis shows the existence of inverse cascade in seismic activity prior to the recent great earthquakes of magnitude 8 or more. This premonitory rise of activity first observed in intermediate-term at large distances, i.e. at the scale of up to 10 sizes of the earthquake source in preparation. In many cases the detailed analysis allows to distinguish a smaller territory, down to the size of the source, where the rise of activity shows intermittent switching from steadily high level to short periods of quiescence. On the background of such intermediate-term rise, episodes of activity, like swarms or sequences of foreshocks could be identified as short-term forerunners of a big earthquake. It is possible that premonitory rise of seismic activity evolves through long, intermediate, short, and immediate, or even nucleation, phases. This is proved statistically for the long and intermediate phases and requires more data for being established at shorter ones.

Introduction. The lithosphere of the Earth is structured as a hierarchical system of volumes of different sizes, from about 10 tectonic plates to about 10^{25} grains of rock (Keilis-Borok 1990). Their relative movement against forces of friction and cohesion happens, to a large extent, through earthquakes. The movement controlled by geometry of volumes and a wide variety of geophysical processes, self-adjusts and concentrates in thin boundary zones between the volumes. Each boundary zone has a similar hierarchical structure, consisting of smaller volumes separated by smaller boundary zones, etc. The hierarchy of volumes along with multitude of processes in the lithosphere suggests a large non-linear system, featuring instability and deterministic chaos as an adequate theoretical description. From this prospective we immediately come to emerging integral empirical regularities of a wide range of similarity, collective behavior, and certain approaches to earthquake prediction.

Except for a few very special sites, like Parkfield in California, earthquakes themselves remain the only observable of the non-linear dynamic system associated with lithosphere, that is recorded systematically over broad territories and times. It is changing now with massive installation of GPS and use of radar interferometer survey, but still none of these compare with seismic networks. Each year about a million of earthquakes with magnitude greater than 2 are registered. None of the top two thousand earthquakes that happen on the Earth each year fall out of the global catalog of earthquakes compiled at the US National Earthquake Information Center (Global Hypocenters Data Base 2000). About a hundred of them are large enough to cause considerable damage. The great earthquakes happen once a year hopefully away from heavily populated areas, but in a decade or two a super catastrophic event occurs.

A particular earthquake cannot be entirely isolated from intrinsically complex dynamics of the lithosphere with evident clustering of events in space and time. That might be an explanation why many researches who concentrate their sight at the source of an earthquake have failed to find a reliable precursor (Wyss 1991). The hierarchical nature of the lithosphere suggests interaction of events at neighbor levels of energy, space, and time. Indeed, large earthquakes usually have numerous aftershocks that cascade energy release from the main shock down the hierarchy. Foreshocks of large earthquakes, if observed, indicate at its last stage the inverse-cascade of energy from seismic background up to the main shock. The occurrence of a relatively large number of intermediate sized earthquakes in northern California prior to the 1906 San Francisco earthquake has been noted (Sykes and Jaume 1990; Bakun 1999). Moreover, Bufe and Varnes (1993) have proposed a power-law increase of seismic rate prior to a major earthquake. These manifestations of the precursory seismic rise of activity at different scales make natural to consider earthquake prediction as consecutive step-by-step reduction of time-space domain where large earthquakes are expected.

In this study we investigate systematically what was in common in seismic activity associated with all the most recent magnitude 8 or greater earthquakes. For this purpose we first consider intermediate-term predictions by algorithms M8 and MSc. Then we search for an evidence of seismic rise at shorter time scales. Finally, we compare aftershock sequences and their statistical properties.

Global seismic activity, 1985-1999. The period is remarkable for a dramatic change in the global seismic energy release that jumped from a stable rate of 2.4×10^{28} erg/yr in 1980-1993 to 7.7×10^{28} erg/yr in 1993-1996. This is slightly less than "the turn of a century" rate of 7.9×10^{28} erg/yr observed for a longer period before 1907. Apparently, in the middle of 1996 the energy release dropped to 4.6×10^{28} erg/yr, i.e. practically the same as observed in 1907-1960. One third of the global seismic energy release in 1985-1999 is due to the ten largest earthquakes listed in Table 1.

Table 1. Magnitude 8.0 or more earthquakes, 1985-1999.

Date and Time	Latitude	Longitude	Depth	Magnitude
1985/09/19 13:17	18.190	-102.533	27	8.1
1986/10/20 06:46	-28.117	-176.367	29	8.3
1989/05/23 10:54	-52.341	160.568	10	8.2
1993/08/08 08:34	12.982	144.801	59	8.2
1994/06/09 00:33	-13.841	-67.553	631	8.2
1994/10/04 13:22	43.773	147.321	14	8.3
1995/04/07 22:06	-15.199	-173.529	21	8.1
1995/12/03 18:01	44.663	149.300	33	8.0
1996/02/17 05:59	-0.891	136.952	33	8.2
1998/03/25 03:12	-62.877	149.527	10	8.3

Seven of them are located within seismic regions of high activity where the annual rate of magnitude 4 or greater earthquakes before 1985 was above 0.4×10^{-4} events per square km. Such an activity is enough to apply without a modification intermediate-term earthquake prediction algorithms M8 and MSc (Keilis-Borok and Kossobokov 1990; Kossobokov et al. 1990) aimed at

magnitude 8.0 or greater events. The other three - 1989 Macquarie Ridge, 1994 Deep Bolivia, and 1998 Balleny Sea – happened in low activity areas of less than 0.1 events per square km. Each of the three was a surprise for seismologists (Special Issue 1994; Wiens et al. 1998), reminding that our knowledge about location of earthquakes remains not 100 per cent complete.

Algorithm M8 was originally designed (Keilis-Borok and Kossobokov 1984) by retroactive analysis of seismicity preceding the greatest, Magnitude 8 or more, earthquakes worldwide, hence its name and our interest to report its performance in predicting the ten earthquakes from Table 1. The scheme of M8 algorithm prediction can be briefly described as follows (Keilis-Borok and Kossobokov 1990; Kossobokov 1997):

Prediction is aimed at the earthquakes of magnitude M_0 and above. We consider different values of M_0 with a step 0.5. The seismic territory is scanned by overlapping circles which diameter $D(M_0)$ equals 384 km, 560 km, 854 km and 1333 km for M_0 = 6.5, 7.0, 7.5 and 8 respectively. Within each circle the sequence of earthquakes is considered with aftershocks removed. The sequence is normalized by the lower magnitude cutoff $M_{min}(\tilde{N})$, $\tilde{N}$ being the standard value of average annual number of earthquakes in the sequence. The magnitude scale we use reflect the size of earthquake sources. For many catalogs this is equivalent to maximal magnitude reported.

Several running averages are computed for this sequence in the sliding time windows to depict different measures of intensity of earthquake flow, its deviation from the long-term trend and clustering of earthquakes. These averages include: the number of the main shocks, N(t); the deviation of N(t) from the long-term trend, L(t); the linear concentration of the main shocks, Z(t); the maximal number of aftershocks (a measure of earthquake clustering), B(t). Each of the functions N, L, Z is calculated for $\tilde{N}$ = 20 and $\tilde{N}$ = 10. As a result, the earthquake sequence is given a robust description by seven averages: N, L, Z (twice each), and B.

"Very large" values are identified for each function using the condition that they are higher than *Q*% of the encountered values.

An alarm or TIP, "time of increased probability", is declared for 5 years, when at least 6 out of 7 functions, including B, become "very large" within a 3-year time window. To make prediction more stable this condition is required for two consecutive moments, t and t + 0.5 years.

The same standard values of parameters are prefixed in the algorithm M8. The running averages are defined in such a robust way, that reasonable variation of parameters does not affect much the prediction results.

Algorithm MSc or "Mendocino Scenario" (Kossobokov et al., 1990) was designed by retroactive analysis of seismicity prior to the Eureka earthquake (1980, M=7.2) near Cape Mendocino in California, hence its name. Given a TIP diagnosed for certain territory **U** at the moment **T,** the algorithm is aimed to find within **U** a *smaller* area **V** where the predicted earthquake has to be expected. An application of the algorithm requires a reasonably complete catalog of earthquakes with magnitudes usually lower than a minimal threshold used by M8. Territory **U** is coarse-grained into small overlapping squares, and the algorithm makes use of seismic activity in each square to outline the area where it shows intermittent switching from steadily high level to short periods of quiescence.

Relation between algorithms M8 and MSc. First, the M8 algorithm makes predictions. Then, each area of alarm is subjected to reduction by the MSc algorithm at the cost that some earthquakes are missed in this second approximation of prediction.

Intermediate-term prediction results. We applied M8, and in the second approximation MSc, in 262 overlapping circles of 667-km radiuses set along the axis of seismic belts. The circles were chosen from a larger number of circles, which scan near-uniformly all the global seismic belts. Therefore, the 262 circles represent all the territories on the Earth where algorithm M8 could be used in its original version. The performance of both M8 and MSc algorithms was reported earlier for the Circum Pacific (Kossobokov et al. 1997, 1999), where the M8 alarms cover on average 31% of its length at any given time, while MSc reduces this number to 9%. All the seven earthquakes of magnitude 8.0 or greater from seismic regions of high activity are predicted by M8 (column M8 of Table 2) and only one of them – 1996 off shore New Guinea - is missed in the second approximation given by MSc (column MSc of Table 2).

Although the low level of background activity does not permit application of the original version of M8, the precursory activation before 1989 Macquarie Ridge and 1998 Balleny Sea earthquakes could be recognized by its modification, when the functions are calculated for $\tilde{N}$ = 1 and 3. The situation with 1994 Great Deep Bolivia earthquake might be somewhat different. It happened at the time of M8 alarm in the standard testing of the algorithm (Healy et al. 1992), at the epicentral distance of 750 km from the center of the circle with the alarm in progress. It would be a premature to attribute preparation processes of the Great Deep Bolivia earthquake to that specific activation of the 1500-km segment that holds the corner of South American seismic belt, although we cannot refute such a possibility due to the scale and uniqueness of the circumstances.

Table 2. M8.0+ earthquakes and associated phenomena.

Date	M8	MSc	Before	Aftershocks
1985/09/19	Predicted	Predicted*	A	65
1986/10/20	Predicted	Predicted	A + Sw4m	205
1989/05/23	Predicted**		A + Eq2w	54
1993/08/08	Predicted	Predicted	A + Eq2m	247
1994/06/09	***		A? + Eq6m	6
1994/10/04	Predicted	Predicted	A + Sw5w	919
1995/04/07	Predicted	Predicted	A + Sw3m	318
1995/12/03	Predicted	Predicted	A + Sw1d	448
1996/02/17	Predicted	Missed	A?	416
1998/03/25	Predicted**		A? + Eq4m	40

Notes: *The region of 1985 Michoacan earthquake allow application of a modified version of the MSc algorithm (Kossobokov et al. 1990). **Modified, "low background rate", version of M8 algorithm applied. ***1994 Great Deep Bolivia earthquake could be associated to the M8 alarm on a shallow part of the South American seismic belt.

Seismic quiescence or rise of activity? The case histories of the ten largest earthquakes of 1985-1999 favor the rise of activity hypothesis. In addition to intermediate-term activation recognized by the M8 algorithm, their majority happens in progress of seismic activation of blocks and faults system at shorter time scale of months or less and at distances comparable to the size of the source. Column Before of Table 2 summarizes our analysis of space versus time diagrams of seismic activity in the corresponding area. An example of such a diagram is given in Fig. 1. It shows distribution of earthquakes from the area of M8 alarm in Kurile Islands (Fig. 2). Vertical axis corresponds to the distance

along seismic belt in km and horizontal axis corresponds to the origin time of an earthquake of magnitude 5 or more. Fig. 1 displays evident absence of quiescence at the approach of 1994/10/04 Shikotan earthquake, although a quiet area, which encountered the future aftershock zone, existed for about a year from March 1993 to April 1994. We mark this activation prior to 1994 Shikotan earthquake with A in column Before of Table 2.

Fig.1. Space-time distribution of earthquakes in the area of 1994/10/04 M8.3 Shikotan and 1995/12/03 M8.0 Iturup earthquakes.

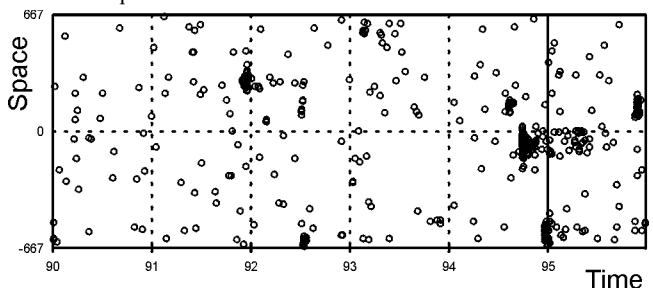

Fig. 2 shows faults of Kurile arc (Geological map of Far East 1970). Its upper plate displays epicenters of all earthquakes of M5.0 or above from the area of M8 alarm in progress before 1994/10/04. Among them a remarkable swarm of six M6.0 or above quakes happened within August 14-30 to the South-West from the straight of Fries, i.e. about a hundred km to the North-East from the future aftershock zone of the October 4 main shock. This manifestation of activation is vividly observed in Fig. 1 as well. That is why we indicate for this earthquake Sw5w in column Before of Table 2 (Sw stands for swarm, 5w – for 5-week separation from the main shock). Next day, on August 31, the epicenter of the magnitude 6.1 earthquake near the southern edge of Kunashir Island outlined the opposite, i.e., southwestern limit of the area ruptured in 1994 Shikotan earthquake. Thus, about a month before the M8.3 main shock two opposite sides of the M8-MS prediction exposed rather unusual activation. The coincidence of the M8-MSc prediction and the aftershock zone is almost exact. According to the NEIC Quick Epicenter Determinations, an apparent M4.5 foreshock occurred at northeastern edge of the future aftershock zone five days before the main shock.

Similar situation is observed for 1995/12/03 Iturup earthquake. Presence of activation, which, for obvious reasons, reflects readjustment after 1994 Shikotan earthquake, and another remarkable swarm of four M6.0 or above events on November 24, 27, 30, and December 2 give us the reason to mark this case with A + Sw1d in Table 2. Note that this swam was also accompanied with a 100-km deep M6.0 earthquake under Kunashir on November 30, which show up the "memory" of the system about the recent, perhaps, "parent" event in October 1994. The M8-MSc prediction was by 50% larger than the actual aftershock zone of 1995 Iturup earthquake (Fig. 2).

We found that each of the ten great earthquakes (Table 2, column Before) occurred at the rise of seismic activity. The question marks for three of them are due to small number of background events, and, to major extent, indicate our cautions rather than absence of activity. In two cases we did not find any "unusual" event - swarm or earthquake – that could be associated with forthcoming rupture zone, but in other eight cases the presence of such event is hardly questionable. Enough to mention the 595-km deep M6.9 earthquake on January 10, 1994 at about 200-km distance from 1994 Great Deep Bolivia one - the previous earthquake of this kind observed there before was in 1963 only.

Fig.2. Epicenters of earthquakes in the area of M8 (shaded gray) and MSc (shaded dark gray) alarms as on July 1994 and July 1995. White dots indicate earthquakes preceding a main shock; black dots indicate their aftershocks. White arrows point to locations of the precursory swarms, black – to the epicenter of a main shock (star).

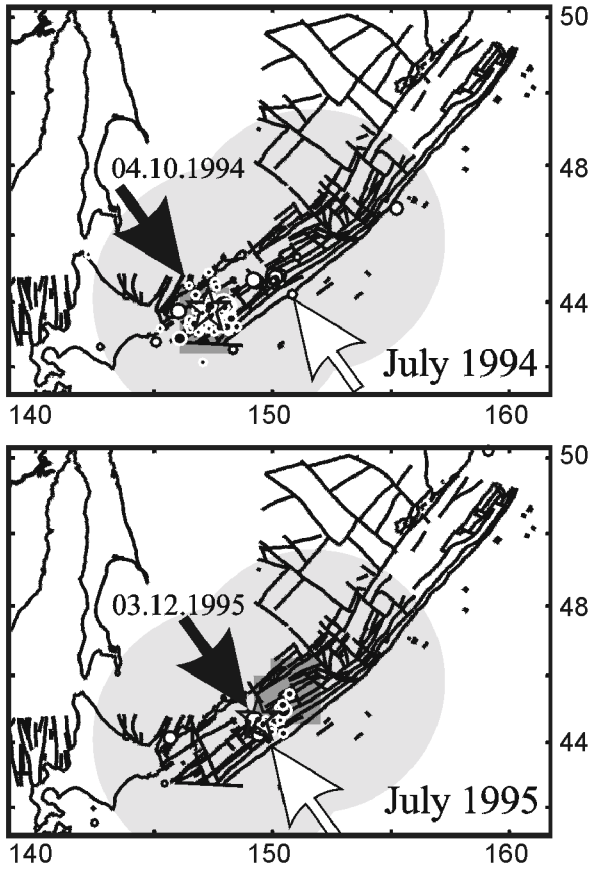

It should be noted that at time scale of days we did not find much foreshocks although all earthquakes with M4.0 or more (Global Hypocenters Data Base, 2000) were considered. Moreover, the only case of a notable "Bufe-Varnes style" power-law increase preceded the above mentioned 1995 Iturup earthquake is due to the swarm of four magnitude 6 events. More data is needed for a conclusive study of seismic activation at this level of specificity.

How the system behaves after the main event? The last column of Table 2 displays the number of M4.0 or above aftershocks determined according to definitions suggested by Molchan and Dmitrieva (1992). Contrary to uniform box-counting approach (Keilis-Borok et al. 1980; Knopoff et al. 1982) of intermediate-term earthquake prediction methods like, e.g. M8, their algorithm uses adaptive game theory for fore-, main-, and aftershock identification and finds the best tradeoff solution between the errors of misclassification.

First, we analyzed each of the ten sequences of aftershocks by inspection of the number versus logarithmic time plot: In a rough

sense, the sequences obey Omori law (Omori 1894) for about 100 days after the main shock. Then we computed the maximum likelihood estimates of parameter values for several formulas representing the decay of occurrence rate of aftershocks with time using the programs by Utsu and Ogata (1997). These programs for statistical analysis of aftershock sequences permit to consider exponential and power-low decays and to make a judgement, which formula of the set is the best fit to the actual data according to the Akaike (1974) information criterion. We found that indeed different versions of Omori law (Omori 1894; Utsu 1961) are better fit than other, e.g. exponential decay (Kisslinger 1996).

However, we should mention several difficulties here. First, many of the ten sequences obey the modified Omori decay with the second main shock separated from the first one by less than 10 days, e.g., for 1994 M8.3 Shikotan earthquake such a separation is 4.77 days. Second, the decay duration and parameter p in the modified Omori law change dramatically, e.g., for 1994 M8.3 Shikotan earthquake $p_1 = 0.91$ and $p_2 = 1.61$, when estimated on the first 100 days after the earthquake. The rate of occurrence did not return to the long-term average in three years. For 1993 M8.2 Guam earthquake $p_1 = 2.01$ and $p_2 = 0.66$, when estimated on the first 50 days after it. At this time the rate of occurrence in the aftershock zone has reached the new stationary level that is 1.5 times higher than the long-term average seismic rate observed before the earthquake. Therefore, it would be a premature to make any final conclusions in the present paper except for a certain claim of complexity that may reflect regional specificity.

Conclusions. Earthquakes, at least the largest observed main shocks, occur after a comparatively large area of lithosphere experiences rise of seismic activity and after smaller earthquakes probe parts of its source. The first happens in intermediate-term scale of years and can be effectively detected by reproducible technique. The existing intermediate-term earthquake prediction algorithms provide limited but, nevertheless, important possibilities to prevent some damage from many catastrophic earthquakes. The second arises in a scale of weeks and shorter. It is hard, if possible, to distinguish this stage of precursory seismic rise without results of the intermediate-term analysis.

Acknowledgements. This study was supported by a subcontract with Cornell University, Geological Sciences, under EAR-9804859 from the US National Science Foundation and administered by the US Civilian Research & Development Foundation for the Independent States of the Former Soviet Union (CRDF). The authors thank Prof. Yosihiko Ogata for source codes of the programs for statistical analysis of aftershock sequences.

References.

Akaike, H., 1974. A new look at the statistical model identification, *IEEE Trans. Autom. Contr.*, AC-19: 716-723.

Bakun, W.H., 1999. Seismic activity of the San Francisco Bay region. *Bull. Seismol. Soc. Am.*, 89, 3: 764-784.

Bufe, C.G., and Varnes, D.J., 1993. Predictive modeling of the seismic cycle of the greater San Francisco Bay region. *J. Geophys. Res.*, 98: 9871-9883.

Geological map of Far East, 1970. Scale 1:2 500 000. Krasnyi, M.L (Ed.).

Global Hypocenters Data Base, 2000. CD-ROM NEIC/USGS, Denver, CO, 1989 and its updates through January 2000.

Healy, J.H., Kossobokov, V.G., and Dewey, J.W., 1992. A test to evaluate the earthquake prediction algorithm, M8. *USGS OFR-401*, 23, Menlo Park, CA.

Keilis-Borok, V.I., 1990. The lithosphere of the Earth as a nonlinear system with implications for earthquake prediction. *Rev. Geophys.* 28, 1: 19-34.

Keilis-Borok, V.I., Knopoff, L. and Rotwain, I.M., 1980. Bursts of aftershocks, long-term precursors of strong earthquakes. *Nature*, 283: 259-263.

Keilis-Borok, V. I. and V. G. Kossobokov, 1984. A complex of long-term precursors for the strongest earthquakes of the world. Proc. 27th Geological congress, 61, Moscow, Nauka: 56-66.

Keilis-Borok, V.I., and Kossobokov, V.G., 1990. Preliminary activation of seismic flow: Algorithm M8. *Phys. Earth Planet. Inter.* 61: 73-83.

Kisslinger, G., 1996. Aftershocks and fault-zone properties. *Advances Geophys.*, 38: 1-36.

Knopoff, L., Kagan, Y. and Knopoff, R., 1982. B-values for aftershocks in real and simulated earthquake sequences. *Bull. Seism. Soc. Am.*, 72: 1663-1675.

Kossobokov, V.,G., 1997. User Manual for M8. In Healy, J.H., Keilis-Borok, V.I., and Lee, W.H.K. (Eds), Algorithms for earthquake statistics and prediction. *IASPEI Software Library, Vol. 6.* Seismol. Soc. Am., El Cerrito, CA.

Kossobokov, V.,G., Keilis-Borok, V.,I. and Smith, S.,W., 1990. Localization of intermediate-term earthquake prediction. *J. Geophys. Res.*, 95: 19763-19772.

Kossobokov, V.G., Romashkova, L.L., Keilis-Borok. V.I. and Healy,J.H., 1999. Testing earthquake prediction algorithms: statistically significant advance prediction of the largest earthquakes in the Circum-Pacific, 1992-1997. *Phys. Earth Planet. Inter.*, 111: 187-196.

Kossobokov,V.G., J.H.Healy, and J.W.Dewey, 1997. Testing an earthquake prediction algorithm. *Pure Appl. Geophys.*, 149: 219-232.

Molchan, G.M., and Dmitrieva, O.E, 1992. Aftershock identification: methods and new approaches. *Geophys. J. Int.* 109: 501-516.

Omori, F., 1894. On the after-shocks of earthquakes, *J. Coll. Sci. Imp. Univ. Tokyo*, 7: 111-200.

Special issue on the great Bolivian earthquake of 1994, *Geoph. Res. Lett.*, 22: 2231-2280.

Sykes, L.M., and Jaume, S.C., 1990. Seismic activity at neighboring faults as a long-term precursor to large earthquakes in San Francisco Bay area. *Nature*, 348: 595-599.

Utsu, T., 1961. A statistical study on the occurrence of aftrshocks. *Geophys. Mag*. 30: 521-605.

Utsu, T., and Ogata, Y., 1997. Statistical analysis of seismicity. In Healy, J.H., Keilis-Borok, V.I., and Lee, W.H.K. (Eds), Algorithms for earthquake statistics and prediction, *IASPEI Software Library, Vol. 6*, Seismol. Soc. Am., El Cerrito, CA.

Wiens, D.A., M.E. Wysession, and L. Lawver. 1998. Recent oceanic intraplate earthquake in Balleny Sea was largest ever detected. *EOS* 79 (July 28): 353.

Wyss, M. (ed.), Evaluation of proposed earthquake precursors, 1991. AGU, Washington, DC.